Journal of Membrane Science & Research

journal homepage: www.msrjournal.com

Research Paper

A New Approach for Fabricating PSf/GO-SiO_2 Membranes with TEOS Modification for Enhanced Oil-Water Separation

Nasir Munasir [1,*], Anis As'adah [1], Ariyanti Rasiana Putri [1], Nuhaa Faaizatunnisa [2], Ezza Syuhada Sazali [3], Ahmad Taufiq [4]

[1] *Department of Physics, Faculty of Mathematics and Natural Sciences, Universitas Negeri Surabaya, Indonesia*
[2] *Department of Chemistry, Faculty of Science and Data Analytics, Institut Teknologi Sepuluh Nopember, Indonesia*
[3] *Department of Physics, Faculty of Science, Universiti Teknologi Malaysia, Malaysia*
[4] *Department of Physics, Faculty of Mathematics and Natural Sciences, Universitas Negeri Malang, Indonesia*

Article info

Received 2025-07-21
Revised 2025-10-20
Accepted 2025-10-22
Available online 2025-10-22

Keywords

Graphene-Membrane
Oil-filtration
Wastewater
SDGs-6
Pollutant organics (oils)

Highlights

- TEOS incorporation optimizes pore structure and hydrophilicity, enhancing separation performance.
- Excess SiO_2 increases membrane thickness and macro-voids, reduce filtration efficiency.
- PSf/GO-SiO_2 membranes demonstrate strong potential for advanced oil-pollutant treatment, although further optimization is required to enhance long-term stability and antifouling capabilities (FRR>93% & FDR ≈4.16%)

Graphical abstract

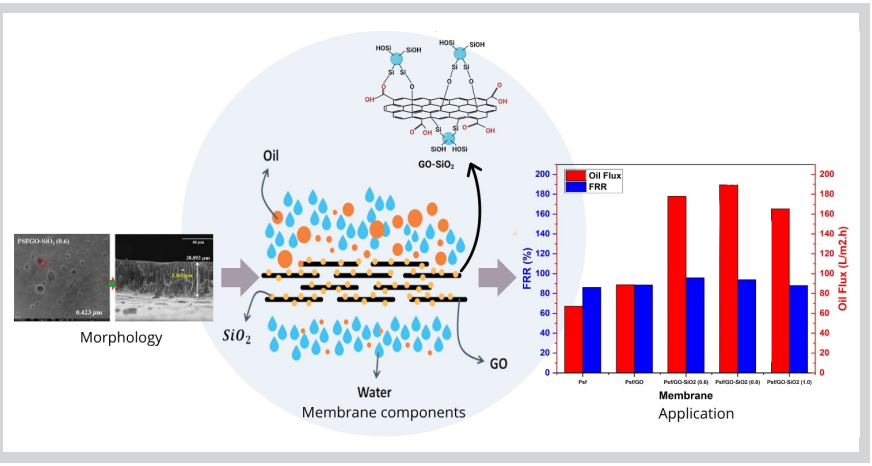

Abstract

Excessive oil pollution is a serious environmental problem because oil and grease are organic substances that are difficult to degrade by bacteria and can cause long-term contamination. One promising solution to overcome this problem is the use of membrane technology. In this study, PSf/GO-SiO_2 membranes were synthesized using various TEOS concentrations via the phase inversion method. Their performance in filtering oil-in-water emulsions was evaluated based on the flux rate (J), flux decline ratio (FDR), and flux recovery ratio (FRR) using a dead-end filtration system. The results showed that the presence of TEOS affected the membrane structure, mainly by changing the pore size, promoting the formation of micro-voids, and increasing the surface hydrophilicity. Among the tested membranes, PSf/GO-SiO_2 with a TEOS concentration of 0.6 showed the best performance, with a pure water flux (Jw) of 185.64 L/m^2.h and a solution flux (Jo) of 177.92 L/m^2.h. The results also showed a small flux reduction (FDR ≈ 4.16%) and high flux recovery (FRR > 95%). However, excessive silica content led to the formation of thicker membranes and decreased filtration efficiency, characterized by an increase in FDR (up to 12%) and a decrease in FRR (≈ 88%). These findings highlight the potential of PSf/GO-SiO_2 membranes for advanced wastewater treatment, while also underlining that the developed membranes have high potential for long-term stability performance and excellent antifouling properties.

1. Introduction

Conventional oil/wastewater treatment methods include chemical, electrochemical, and biological approaches. For instance, peroxi-coagulation and peroxi-electrocoagulation have demonstrated efficient dye and pollutant removal but involve high energy consumption and chemical dosing, which may limit large-scale applications [1]. Electro-oxidation processes are effective for treating petroleum refinery wastewater, though the operational

* Corresponding author: munasir_physics@unesa.ac.id (N. Munasir)

DOI: 10.22079/jmsr.2025.2057559.1720

cost and electrode fouling remain concerns [2]. Biological systems such as fixed-bed biofilm reactors with optimized biofilm carriers are eco-friendly but require long hydraulic retention times and are sensitive to operational conditions [3]. The Chemical, electrochemical, and biological methods can treat oil-contaminated wastewater but often face challenges such as high energy use, chemical demand, operational costs, and long retention times. Membrane-based separation offers a scalable, efficient, and sustainable alternative for oil–water treatment and pollution control, providing a physical barrier for effective oil rejection along with modular operation and easy scalability, making it an attractive option for sustainable wastewater management and oil pollution mitigation [1]. In the present era, industrial growth leads to less favorable environmental conditions. Water pollution from oil generally arises due to the swift expansion of industries involved in oil and gas, metallurgy, and food [4]. Oil particles in water can corrode pipes, block water channels, and disrupt ecosystems. Consequently, they can adversely affect human health and metabolism, while also disturbing the ecological balance by altering the mineral composition of clean water and reducing soil fertility [5,6]. According to the BPS data (2019), the yearly consumption of mustard cooking oil has consistently increased. In 2018, it amounted to 10.79 liters/capita/year, with an increase of 11.38 liters/capita/year in 2020. Cooking oil that is used repeatedly has a negative impact on the body. This is because it contains carcinogens, acids, and high peroxide numbers that can trigger cancer.

Membranes are among the most widely used wastewater treatment methods [7]. Membranes are becoming a widely used filtration technology in industries such as chemical, petrochemical, food, pharmaceutical, cosmetics, water desalination, water and wastewater treatment [8,9]. The use of membrane filtration technology was chosen because it has the characteristics of high efficiency, energy saving, simple operation, environmental protection, and fast processing [10,11]. Membranes are semipermeable, allowing the separation of substances based on molecular size and shape. However, retained particles on the membrane surface can cause adhesion, leading to fouling. Good hydrophilicity helps reduce this adhesion, increases water flux, and lowers the risk of fouling by forming a protective water layer on the membrane surface. Additionally, the high surface energy of hydrophilic membranes helps repel hydrophobic particles such as oil [8,12].

The membrane separation performance of oil in water is affected by the nature of the feed solution, operational pressure, and oil particle size. The particle size of oil in water ranges from < 20 μ m, where the oil-in-water mixture has a continuous phase of water and a dispersed phase of oil [10,13]. Ebrahimi et al. reported that the PAN/GO-SiO_2 membrane was successfully fabricated using the electrospinning method [14]. The results indicate poor membrane wettability, as shown by a low water flux value of 21 L/m²·h. This is likely due to syringe blockage caused by the excessive addition of SiO_2. In contrast, the membrane demonstrated a relatively high vegetable oil rejection of 90%. Similarly, Liu et al. [15] reported that cellulose acetate membranes coated with SiO_2-GO exhibited increased surface roughness and improved hydrophilicity, as indicated by a contact angle of 25°, a water flux of 875 L/m²·h, and an oil rejection rate of 99.4%. These findings reflect the strong hydrophilic nature of the membrane, which effectively inhibits oil particle adhesion on the surface. Polysulfone is one of the polymers used in membrane manufacturing [16].

Polysulfone has advantages such as good chemical and operating temperature resistance, tunable pores, high mechanical strength, and low cost due to its reusability [17]. In water treatment applications, the natural hydrophobic nature of polymer membranes often limits their performance. To overcome this problem, membrane modification is necessary to improve the membrane hydrophilicity and efficiency by incorporating inorganic materials or nanomaterials into the membrane matrix [18]. Incorporation involving the addition of nanoparticles or inorganic additives has been shown to not only improve water permeability but also help minimize environmental and fouling problems [19]. Graphene Oxide (GO) is a two-dimensional carbon-based material with a layered structure consisting of sp^2 and sp^3 hybridized carbon atoms [20]. This structure is further enriched with various oxygen-containing functional groups, which makes GO inherently hydrophilic [21,22]. The hydrophilic nature of GO originates from the presence of oxygenated groups along its surface, which can form strong hydrogen bonds with water molecules, thereby increasing the membrane's affinity for water. Nguyen et al [17] reported that the addition of GO into the polysulfone matrix can increase the hydrophilicity of the membrane with a reduced contact angle value of up to 76.2°. This enhancement in water affinity not only promotes higher water flux but also improves overall membrane permeability. Moreover, membrane performance is influenced not only by the chemical properties of the surface but also by structural changes, such as an increase in pore size, which play a crucial role in determining its practical applications. The use of silica (SiO_2) is often chosen as an additive in membrane fabrication. Known for its stable, porous structure, SiO_2 contributes to improved separation and purification capabilities [23]. Structurally, silica is composed of interconnected SiO_4 tetrahedra, forming a three-dimensional network that enhances both the mechanical and filtration properties of the membrane. Naturally occurring silica is found in sand, glass, and rocks. Silica possesses beneficial properties such as a large surface area, strong adsorption capacity, high surface energy, chemical stability, and excellent dispersion. Additionally, SiO_2 is inherently hydrophilic due to its good dispersibility in water [24]. These characteristics, particularly its hydrophilicity, chemical stability, and ease of preparation, make SiO_2 an ideal additive for polymer membrane enhancement [25]. The hydrophilic functional groups on the surface of SiO_2 particles contribute to improved water permeability and enhanced antifouling properties of membranes [26]. Huang et al. demonstrated that incorporating 5 wt% SiO_2 into a polysulfone membrane reduced the contact angle to 66.4°, confirming increased hydrophilicity and wettability. Furthermore, the addition of silica also led to an increase in membrane porosity [27].

In this study, a new approach was introduced for fabricating PSf/GO–SiO_2 hybrid membranes by utilizing TEOS as a silica precursor through an *in-situ* hydrolysis process. Unlike previous studies that relied on direct blending of preformed SiO_2 nanoparticles, the *in-situ* formation of SiO_2 within the GO network ensures better dispersion, stronger interfacial interaction, and enhanced compatibility with the PSf matrix. This approach addresses a major challenge in earlier works related to nanoparticle agglomeration and poor phase stability. By systematically varying the TEOS concentration, this work elucidates the relationship between surface chemistry, hydrophilicity, and membrane microstructure, leading to improved water flux and oil rejection efficiency. The findings highlight a practical strategy for designing high-performance hybrid membranes for sustainable oily wastewater treatment.

2. Materials and Methods

2.1. Materials

Graphite powder (< 20 μ m, Sigma-Aldrich), potassium permanganate ($KMnO_4$, 99%), sodium nitrate ($NaNO_3$), hydrogen peroxide (H_2O_2) (30%, Merck), hydrochloric acid (HCl) (37%, Merck), sulfuric acid (H_2SO_4) (95%-97%, Merck), ethanol (C_2H_5OH, 99.7%), tetraethyl orthosilicate (TEOS) (Sigma-Aldrich), ammonia (NH_4OH) (25%, Merck), polysulfone (PSf) (Sigma-Aldrich), *N,N-Dimethylacetamide* (DMAc) (Merck), and used cooking oil.

2.2. Synthesis of GO

Graphene Oxide (GO) was prepared following Hummers' method [28]. A total of 5 g of graphite powder was added to a mixture of 2.5 g $NaNO_3$ and 120 mL concentrated H_2SO_4. The mixture was stirred in an ice bath for 30 min. After that, 15 g K_2MnO_4 was added dropwise to the mixture and stirred for 30 min until homogeneous. The solution was left at room temperature for 3 hours, until a purple suspension began to form. Then, 150 mL of distilled water was added with stirring and then heated at 95–100°C for 3 hours. Then, 50 mL H_2O_2 was added and stirred for 10 min. The solution was washed several times with 1 M HCl and distilled water until the pH was neutral. The resulting solid was then separated by centrifugation and dried at 60 °C for 6 hours. A schematic representation of the synthesis of GO from graphite powder is shown in Fig. 1.

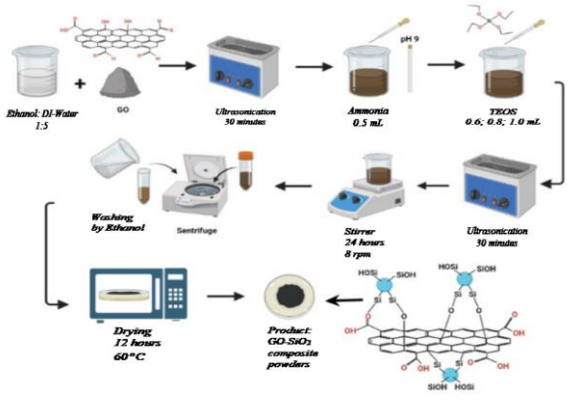

Fig. 1. The synthesis of GO material from graphite.

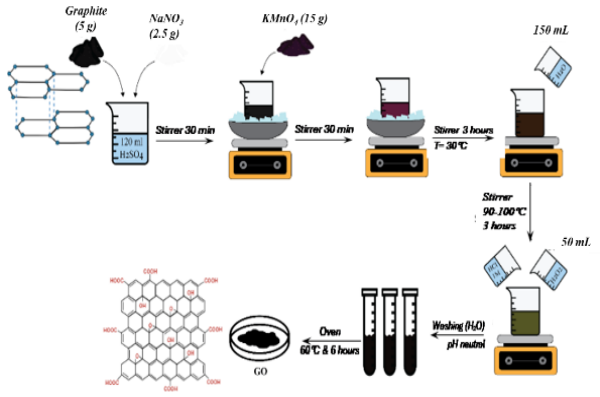

Fig. 2. Synthesis steps of the GO–SiO_2 composite material.

2.3. Synthesis of GO-SiO_2

GO-SiO_2 composites were synthesized through an in situ hydrolysis method, with slight modifications from the research of Angesti et.al. [28]. A total of 0.0125 g of GO powder was dispersed in 150 mL of a mixture of ethanol: distilled water with a ratio of 1:5. The mixture was sonicated for 30 min to achieve homogenization. A total of 0.5 mL of ammonia was added to adjust the pH of the solution to 9. Next, variations in the addition of TEOS were added with a mass ratio of 0.6, 0.8, and 1.0 mL, and sonicated for 30 min. The mixture was stirred at room temperature for 24 hours. The sample was washed with technical ethanol and separated by centrifugation. The solid was dried at 60°C for 12 hours. The synthesis process of GO-SiO_2 is illustrated in Fig. 2.

2.4. Preparation of Psf/GO-SiO_2

The PSf, PSf/GO, and PSf/GO-SiO_2 membranes were fabricated using the phase inversion technique [28]. A total of 0.0333 grams of GO and GO-SiO_2 (membrane fillers) were dissolved in PSf and DMAc (membrane matrix) and mixed until the mixture became homogeneous. This membrane solution was designated a 0.5% wt membrane.

The PSf was dissolved in DMAc using a hot plate stirrer for 3 hours at room temperature, and the fillers were subsequently homogenized through sonication for 30 min at room temperature. The resulting membranes were then immersed in a coagulation bath containing distilled water for 24 hours. The PSf/GO-SiO_2 membrane samples with varying TEOS concentrations (0.6, 0.8, and 1.0 mL) were designated as PSf/GO-SiO_2(0.6), PSf/GO-SiO_2(0.8), and PSf/GO-SiO_2(1.0), respectively. Fig. 3 illustrates the fabrication process of PSf membranes and PSf composite membranes with GO and GO-SiO_2 using the phase inversion technique.

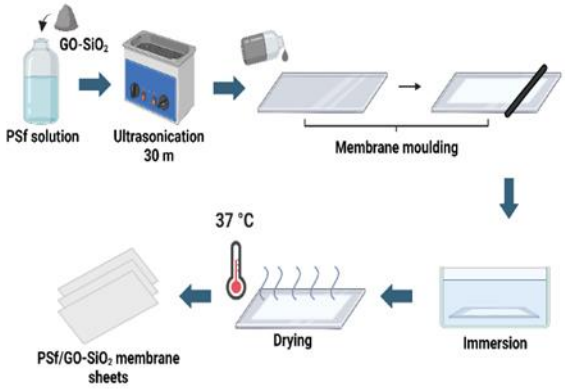

Fig. 3. Fabrication steps of silica-modified graphene membranes.

2.5. Oil Pollutants Preparation

Preparation of the primary solution of oil pollutants was conducted by mixing oil and water. The concentration of the solution used was 1000 mg/L, as much as 0.1 g of used palm oil in 100 mL of distilled water. The manufacturing process was carried out with a mixture in sonication for 20 min and continued with a stirrer for 9 hours at high speed. For the filtration process used a concentration of 50 mg/L. The filtration system used was dead-end filtration. The membrane area used during the test was 16 cm^2 and the vacuum pump pressure was 675 mmHg. The flux J ($Lm^{-2}h^{-1}$) was calculated using equation (1), which passed through the feed solution for 30 min.

$$J = \frac{V}{At} \tag{1}$$

where, V is the permeate volume, A is the effective area of the membrane, and t is the filtration time. The membrane rejection rate (R) for used oil in water was calculated from equation (2) using a 30 ml oil-in-water sample.

$$R = \left(1 - \frac{C_p}{C_f}\right) \times 100\% \tag{2}$$

Permeate concentration (C_P), the concentration of the contaminant (e.g., oil) in the permeate solution after filtration. This value indicates the residual pollutant level in the water that has passed through the membrane. Feed concentration (C_f), the concentration of the contaminant (e.g., oil) in the feed solution before filtration begins.

Another crucial parameter for assessing membrane performance in filtration processes is the Flux Decline Ratio (FDR) and the Flux Recovery Ratio (FRR). The FDR quantifies the extent of flux reduction caused by fouling as shown in equation (3); a higher FDR value indicates more severe fouling and thus a decline in membrane performance. Here, J_w refers to the pure water flux prior to fouling, whereas J_0 denotes the flux measured after the filtration of the oil–water emulsion. Qualitatively, the FDR exhibits a similar trend to the oil rejection (%). In contrast, the FRR reflects the membrane's ability to restore its flux after fouling; a higher FRR indicates superior antifouling properties and more effective flux recovery as shown in equation (4).

$$FDR = \left(1 - \frac{J_o}{J_w}\right) \times 100\% \tag{3}$$

$$FRR = \frac{J_o}{J_w} \times 100\% \tag{4}$$

In this study, palm oil was used as the oil source, selected based on its availability, environmental relevance, and widespread presence in oily industrial wastewater, particularly from the food and agro-industrial sectors. Although fatty acid emulsions are chemically simpler and more stable, palm oil more accurately represents real wastewater conditions, which typically contain complex triglyceride-based oils.

2.6. Characterizations

The crystal structure of GO and GO-SiO_2 particles was characterized by X-Ray Diffraction (XRD) (an X'Pert MPD Diffractometer) using Cu-Ka radiation (λ = 1.5406 Å). Functional groups were characterized by Fourier Transform Infrared (FTIR) spectra using a Shimadzu type IR Prestige-21 (Kyoto, Japan) at wavelengths of 500-4000 cm^{-1}. Raman spectroscopy with a single Raman spectrum (532 nm laser) (LabRAM HR Evolution) was used to characterize the carbon framework of the samples. The hydrophilicity of the membrane was determined by contact angle measurement using the sessile drop technique (Goniometer LSB-1800B). The surface morphology and cross-sectional structure of the membrane were characterized using a Scanning Electron Microscope (SEM). The oil concentration in the solution was analyzed using a UV-Vis spectrophotometer.

3. Results and Discussion

3.1. XRD Pattern of GO and GO-SiO_2

X-Ray Diffraction (XRD) characterization was used to determine the diffraction patterns of GO and GO-SiO_2 composites. The results of XRD characterization of GO and GO-SiO_2 are shown in Fig. 4. Based on the diffractogram results, it shows that the GO-SiO_2 composite gives rise to absorption peaks for GO and SiO_2. The absorption diffraction peak of GO was identified at an angle of 2θ = 10.22°, which had an amorphous crystal pattern with a Miller index (002). This peak indicates that strong oxidation occurs in graphite, thereby reducing the degree of graphite crystallization, where the graphite diffraction peak is 26.5° [29]. Meanwhile, the GO-SiO_2 composite shows a shift in the diffraction peak in the angular range of 2θ = 11°, this shift remains close to the characteristic diffraction peak of GO and shows that the intercalation between GO sheets does not produce major changes [30]. The appearance of a SiO_2 diffraction peak with increasing intensity as TEOS varies, seen at 2θ = 24º[31]. This peak shows the

appearance of amorphous SiO_2, which has bonded to the GO surface, where this result is in line with the research of Dong *et al*. [29]. The appearance of the SiO_2 diffraction peak in the composite indicates that the synthesis of the GO-SiO_2 composite was successful.

3.2. FTIR Spectral Analysis of GO and GO-SiO_2

The results of FTIR characterization of GO and GO-SiO_2 are shown in Fig. 5 with the wavenumber range is 500-4000 cm^{-1}. The FTIR spectrum of GO shows an absorption band at wave number 1049.32 cm^{-1} which indicates the presence of symmetrical tensile vibrations of the epoxy functional group (C-O). At a wave number of 1626.20 cm^{-1}, vibrations of aromatic group bonds (C=C) in the graphite structure and absorption of water molecules are generated. while the absorption bands at wave numbers 1719.61 cm^{-1} and 3416.08 cm^{-1} indicate the vibration of the carboxyl group (C=O), and the stretching vibration of the hydroxyl group (-OH) of the H_2O water molecule. These results confirm the presence of the main functional groups of GO that appear, namely hydroxyl, carboxyl, epoxy and aromatic groups [32,33].

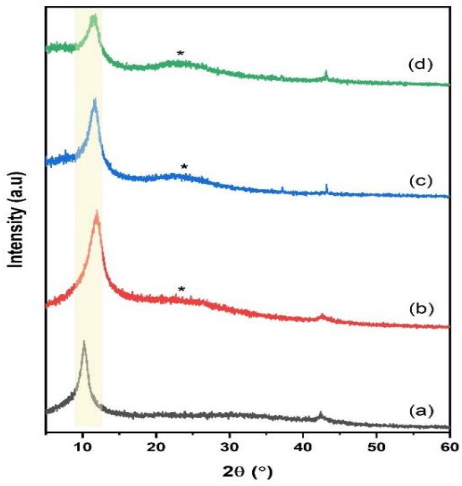

Fig. 4. Pattern diffraction: (a) GO, (b) GO-SiO_2#(0.6), (c) GO-SiO_2#(0.8), and (d) GO-SiO_2#(1.0).

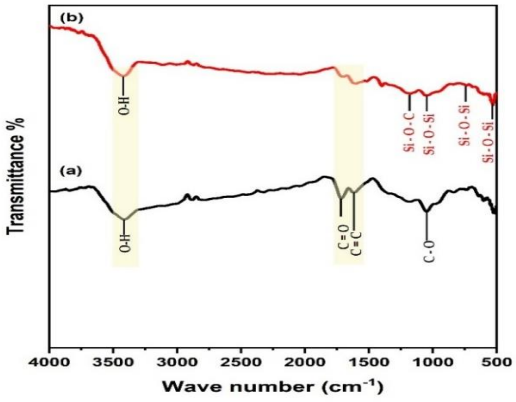

Fig. 5. FTIR spectra: (a)GO and (b) GO-SiO_2#(0.6).

The FTIR spectrum of the GO-SiO_2 composite presents the absorption band at the wavenumber of 737.80 cm^{-1} showing symmetrical vibrations of the siloxane group (Si-O-Si). Furthermore, the presence of SiO_2 at 1054.14 cm^{-1} also indicates the presence of vibrations asymmetric (Si -O-C). These results prove that silica (SiO_2) and GO have been combined through a hydrolysis process, as evidenced by the presence of an absorption band at a wavenumber of 3427.65 cm^{-1} which gives rise to absorption from hydroxyl groups (-OH) originating from water. Based on these results, the FTIR spectrum of the GO-SiO_2 composite shows the characteristics of the main functional groups, namely hydroxyl, siloxane, and silanol[34,35].

3.3. Raman Spectra of GO and GO-SiO_2

Raman spectroscopy characterization is used to identify the purity and defects of a material. The D peak indicates structural defects or lattice disorder, while the G peak corresponds to sp^2 carbon vibrations. The results of the Raman characterization are shown in Fig. 6. Raman results show that GO samples have D and G peaks at 1349.82 cm^{-1} and 1602.54 cm^{-1}, respectively. Meanwhile, the GO-SiO_2 composite sample has D and G peaks at 1346.76 cm^{-1} and 1602.54 cm^{-1}, respectively. The wavenumber shift in the band is caused by charge transfer between GO and SiO_2 [36]. The I_D/I_G ratio values for GO and GO-SiO_2 samples are 1.04 and 1.02, respectively. The larger I_D/I_G ratio value of GO indicates that the GO sample does not cause large defects in the structure of the new material. In addition, the peaks of both samples have no significant changes and indicate that SiO_2 is connected with GO through covalent bonds.[29].

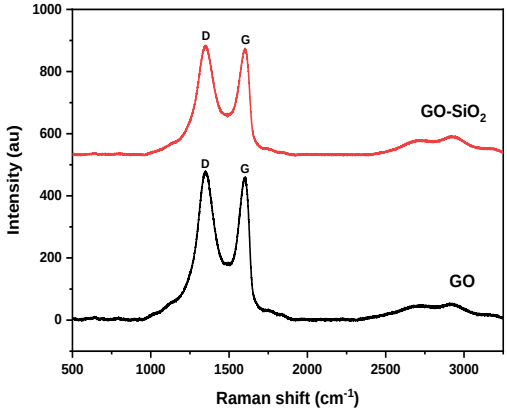

Fig. 6. Raman spectra of GO and GO-SiO_2.

3.4. Morphology of Membrane Psf/GO-SiO_2

In order to obtain membranes with good performance in certain applications, it is necessary to manipulate the morphological structure of the membrane. Surface and cross-sectional morphological structures of the membrane were observed using SEM. The cross-sectional structural characterization (Fig. 7) shows that the membrane has finger-like macrovoids, a typical morphology of asymmetric membranes formed when high-viscosity polymer solutions are displaced by low-viscosity non-solvents during phase inversion [37]. Incorporating various inorganic nanoparticles into polyethersulfone ultrafiltration membranes has been shown to significantly enhance membrane hydrophilicity, water flux, and protein rejection efficiency, with BSA rejection rates reaching up to 98.5%, demonstrating the effectiveness of nanoparticle additives in improving membrane performance [35]. Similarly, in this study, structural modification through the addition of SiO_2 (Fig. 7(c–d)) resulted in noticeable changes in membrane thickness, where excessive SiO_2 led to agglomeration within the membrane matrix, contributing to increased thickness and potentially affecting membrane permeability[17]. The red circles in Fig. 7 and 8 highlight the presence of lumps or inhomogeneous spots on the surface of the pure PSf membrane. These are not caused by nanoparticles, but by residual DMAc solvent that was not completely dissolved or distributed evenly during the phase inversion process. This explains why the PSf surface texture appears less smooth than composite membranes modified with GO or GO-SiO_2.

Furthermore, Fig. 8 shows the surface morphology of the membrane. The modification of the membrane structure shows the difference in pore size, which is getting bigger. The presence of clumps on the surface of the PSf membrane (Fig. 8(a)) indicates that there is DMAc material that is still not completely dissolved. Then, there is a sheet-shaped distribution of GO on the surface of the PSf/GO membrane (Fig. 8(b)). The structural modification of the PSf/GO-SiO_2 membrane (Fig. 8(c-d)) also shows the agglomeration of SiO_2. The addition of GO and SiO_2 to the membrane is able to increase the membrane pore size [8]. Moreover, with a higher amount of added SiO_2, the SiO_2 grains become more visible on the membrane surface and can agglomerate in the pores, leading to pore clogging [36].

3.5. Surface Wettability of Membrane Psf/GO-SiO_2

Surface wettability can be determined through contact angle measurements. Hydrophilic membranes have high surface wettability characterized by very low contact angle values. Hydrophilic membranes exhibit contact angles below 90°, whereas hydrophobic membranes have contact angles above 90°. Measurements were made using a Contact Angle Goniometer instrument at room temperature and using a 20 µL micropipette.

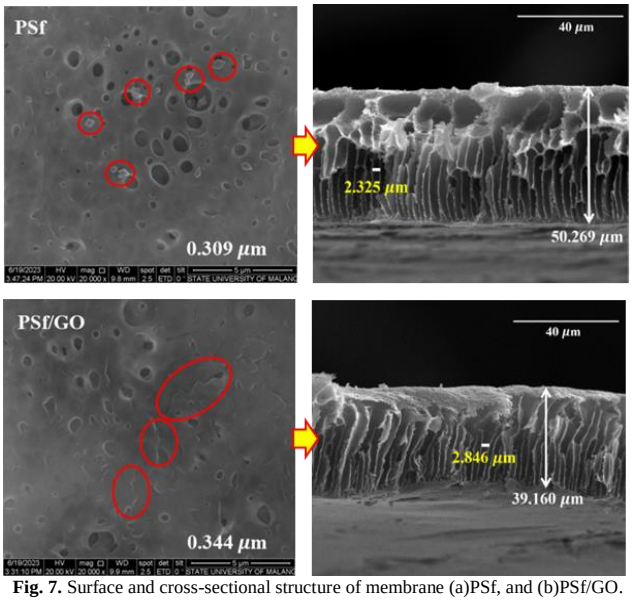

Fig. 7. Surface and cross-sectional structure of membrane (a)PSf, and (b)PSf/GO.

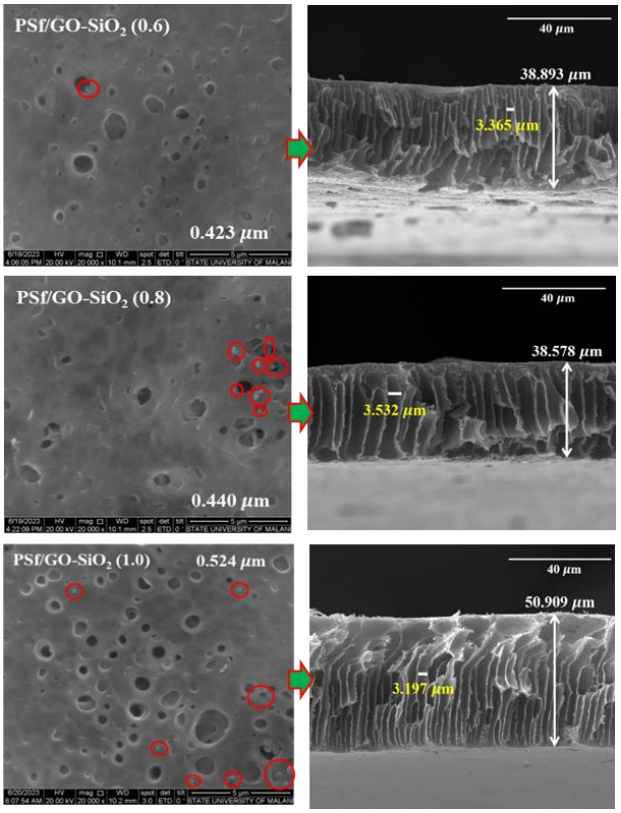

Fig. 8. Surface and cross-sectional structure of membrane PSf/GO-SiO_2 (#0.6), PSf/GO-SiO_2 (#0.8), and PSf/GO-SiO_2 (#1.0).

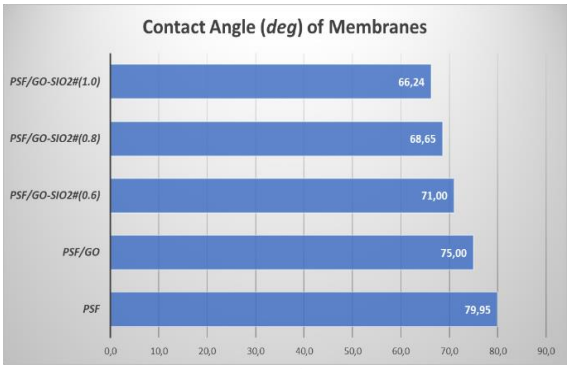

Fig. 9. Water contact angle of the materials membrane.

Fig. 9 presents the contact angle measurements of the membrane. It is evident that the contact angle decreases with the incorporation of SiO_2 nanoparticles. This reduction indicates an enhancement in the membrane's hydrophilicity. The improved hydrophilic behavior arises from the hydroxyl groups (–OH) present on the SiO_2 surface, which increase the number of hydrophilic sites within the membrane. In addition, the incorporation of SiO_2 can enhance porosity and alter the surface morphology, thereby facilitating the spreading and interaction of water molecules with the membrane [15].

Based on the Contact Angle test results (Fig. 9), it can be observed that the contact angles of the PSf, PSf/GO, and PSf/GO-SiO_2 membranes with varying TEOS concentrations (0.6, 0.8, and 1.0 mL) are 79.95°, 75.00°, 71.00°, 68.65°, and 66.24°, respectively. The contact angle plays a crucial role in influencing membrane performance and provides insight into the surface properties of the membrane. This test indicates that as the SiO_2 content increases, the membrane contact angle decreases, leading to enhanced membrane hydrophilicity[12]. The increased membrane hydrophilicity value will result in increased flux, which is caused by the strong membrane affinity for water molecules [33]. The presence of many hydroxyl groups on the membrane surface can increase its hydrophilic properties[12]. Furthermore, the integration of GO (hydrophilic) will strengthen the attraction effect and SiO_2 also contributes to increasing the hydrophilicity of the membrane more towards the hydrophilic surface, due to the inorganic structure of silica [33]. Increasing SiO_2 content decreases the contact angle, indicating enhanced hydrophilicity of the membrane. The results of the contact angle test of the PSf/GO-SiO_2 membrane are in accordance with those previously reported by Liu *et al.* [15], who also reported that increasing the SiO_2 content causes a decrease in the contact angle, and increases the hydrophilicity of the membrane.

3.6. Filtration Performance of Membrane Psf/GO-SiO_2

Membrane application for oil-contaminated water filtration was carried out with a concentration of 100 ppm on a vacuum pump with a pressure of 675 mmHg. PSf/GO-SiO_2 membrane with an active surface area of 0.0009 m^2 was applied for filtration in 20 mL of water+oil pollutants. The membrane flux value was determined using equation (1). For instance, flux values of 67.21 L/m^2·h, 88.86 L/m^2·h, and 177.92 L/m^2·h were obtained for PSf, PSf/GO, and PSf/GO-SiO_2 (0.6) membranes, respectively. These results indicate that the addition of SiO_2 can increase the flux and enlarge the pore size of the membrane. Membranes with large pores will allow faster filtration. However, the increasing addition of SiO_2 will be able to provide good total membrane flux performance [33].

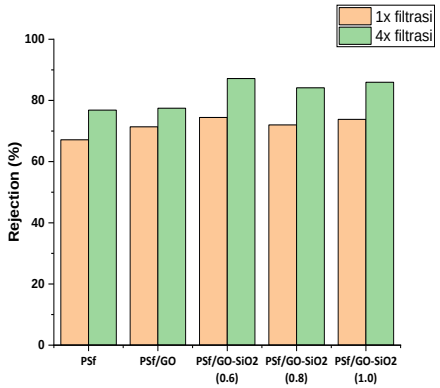

Fig. 10. Oil pollutant rejection performance using filtration.

SiO_2 nanoparticles serve as a support layer to facilitate increased flux the GO layer acts as a shield to inhibit the accumulation of various contaminants, as reported by Li *et al.* [25], silica nanoparticles function as a supporting layer that facilitates increased flux. In contrast, the GO layer acts as a shield to inhibit the accumulation of diverse contaminants The integration of GO and SiO_2 in the composite membrane offers important benefits, such as increased separation efficiency and improved resistance to fouling. The rejection rates during filtration were determined using equation (2) with the results illustrated in the Table 2.

The calculated data of this study, using equation 1-4, and Table 1, can be used to represent the membrane performance, especially the oil rejection capability or flux decline ratio due to fouling (FDR) and the ability to recover performance after fouling (FRR), as in Table 2. The results of the analysis of each membrane sample are as follows: (i) the Psf membrane shows relatively high fouling, as representing the baseline performance of the PSf membrane; (ii) the Psf/GO membrane shows improved antifouling performance due to

the incorporation of GO; (iii) the Psf/GO-SiO_2(0.6) membrane shows excellent antifouling performance, minimal flux decline is observed; (iv) the Psf/GO-SiO_2 (0.8) membrane shows stable performance with low fouling tendency; and (v) for the Psf/GO-SiO_2(1.0) membrane antifouling decreases, possibly because pores begin to enlarge, or the surface becomes less homogeneous as an effect of the addition of excess SiO_2. Therefore, from these analysis, it shows that the performance of the Psf/GO-SiO_2(0.6) membrane shows the best antifouling performance.

Table 1
Experimental data of membrane Flux.

Membrans	Pure Water		Oil Pollutants	
	t (h)	J_w (L/m².h)	t (h)	J_0 (L/m².h)
PSf	0.24	78.125	0.279	67.21
PSf/GO	0.187	100.267	0.211	88.86
PSf/GO-SiO_2#(0.6)	0.101	185.643	0.159	177.92
PSf/GO-SiO_2#(0.8)	0.093	201.613	0.157	189.43
PSf/GO-SiO_2#(1.0)	0.136	187.868	0.178	165.34

Table 2
Data analysis of membrane performance.

Membranes	Water flux, J_w (L/m².h)	Oil flux, J_0 (L/m².h)	FDR (%)	FRR (%)
PSf	78.13	67.21	13.96	86.04
PSf/GO	100.27	88.86	11.38	88.62
PSf/GO–SiO_2(0.6)	185.64	177.92	4.16	95.84
PSf/GO–SiO_2(0.8)	201.60	189.43	6.04	93.96
PSf/GO–SiO_2 (1.0)	187.87	165.34	12.00	88.00

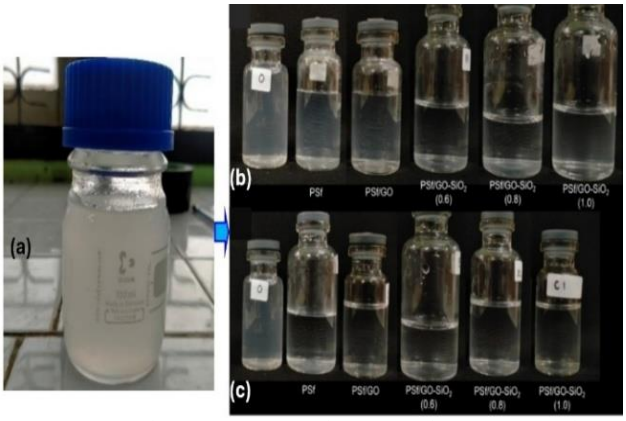

Fig. 11. Visual result of oil–water separation after dead-end filtration using the fabricated membrane.

Despite improvements in rejection rate across repeated filtrations, the overall rejection levels remained comparatively moderate. This outcome is likely attributed to various factors that impact membrane filtration performance, such as operating pressure, pore size, particle dimensions, and electrostatic interactions. Electrostatic interactions—referring to charge-based interactions between the membrane surface and suspended particles—play a vital role in enhancing the membrane's contaminant separation capabilities. In accordance with research reported by Ullah *et al.* (2021), electrostatic repulsion can increase particle rejection efficiency [38]. The results obtained show a trend of increasing oil contaminant removal efficiency, which is characterized by a significant increase in rejection performance, especially in membranes combined with GO-SiO_2. The role of SiO_2 in the membrane can increase membrane selectivity. Sjahriza and Herlambang (2021) [26] reported that smaller silica particle sizes can affect membrane performance due to their wide pore diameter. This finding is consistent with the report by Rezaee *et al.* [39], which stated that the addition and modification of inorganic materials such as SiO_2 in the polymer matrix can enhance both the selectivity (rejection) and permeability of the membrane.

Therefore, the combination of the two materials into a GO-SiO_2 composite as a filler in the PSf matrix provides high separation efficiency due to the high rejection value. During the filtration process, oil-contaminated water is retained in the membrane; this can cause the accumulation of water molecules on the membrane surface and increase the rejection performance. The rejection itself can be influenced by the nature and size of the pores in the membrane, the higher the pores, the easier it is for substances to pass through the membrane [33]. The experimental results show that the modification of the PSf membrane with graphene oxide (GO) and SiO_2 nanoparticles further improves its rejection performance (Fig. 10 and Fig. 11).

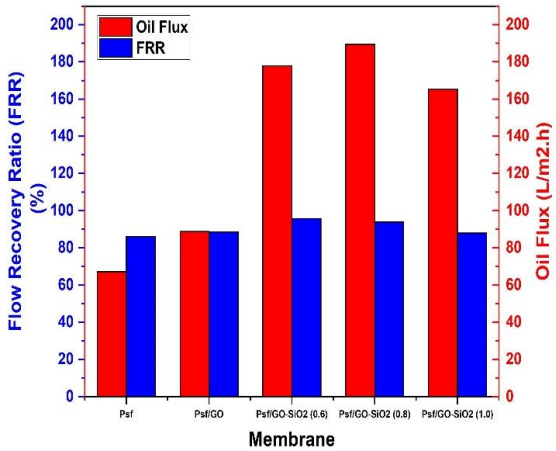

Fig. 12. Membrane flux and FRR (%) results graph for oil pollutants.

Flux refers to the volume of liquid that passes through a membrane per unit area in a given time. The flux performance of the membranes is illustrated in Fig. 12. Among the tested samples, the PSf/GO-SiO_2#(0.8 mL) membrane exhibited the highest flux, reaching 201.613 L/m²·h for pure water and 119.427 L/m²·h for the feed solution. A higher flux typically reflects better membrane hydrophilicity. This improvement is largely attributed to the incorporation of graphene oxide (GO), which introduces hydroxyl groups that enhance water affinity compared to the unmodified polysulfone (PSf) membrane [17]. In addition, the higher addition of SiO_2 also increases hydrophilicity [25]. However, further increasing the SiO_2 content—as in the PSf/GO-SiO_2#(1.0) membrane—resulted in a decline in flux. This is likely due to increased membrane thickness, which can impede water transport and lower the flux rate. Specifically, the pure water flux (PWF) value was consistently higher than the permeate flux from the feed solution. This significant difference can be influenced by the concentration and viscosity of the feed solution. High viscosity decreases the diffusion of the solution, making it more difficult for the fluid to pass through the membrane gap. This can cause the solid layer and pores on the membrane surface to become clogged, leading to fouling [40].

The negative zeta potential of GO can also be attributed to the ionization of epoxy and hydroxyl functional groups, as reported by Li *et al.* [44]. In this study, the resulting membrane had a negative surface charge due to the presence of GO in the membrane, which can enhance the filtration process. This is due to the low pressure that can enhance the antifouling properties. This property is formed from the negative charge and high hydrophilicity of the membrane. The addition of SiO_2 to the membrane and GO demonstrated an increase in hydrophilicity and surface area due to the abundant hydroxyl groups that contribute to the formation of a hydrophilic membrane [45]. Used cooking oil is neutrally charged and contains peroxides as well as saturated fatty acids. It consists of hydrocarbon compounds with covalent bonds between carbon and hydrogen atoms, resulting in non-polar characteristics [46]. Repeated use of cooking oil leads to oxidation processes and potential contamination with metal ions from frying pans. However, the presence of metal ions in used cooking oil has not been extensively discussed in previous studies. The neutral charge of the oil implies that the filtration process in this study primarily depends on oil particle size. The particle size of oil in an oil-in-water solution is typically < 20 μm [13]. An illustration of the oil-in-water filtration mechanism is provided in Fig. 13. The low rejection percentage observed in this study suggests that extremely small oil particles may pass through the membrane pores. The PSf/GO-SiO_2 membrane fabrication method is cost-effective, scalable, and environmentally friendly, using readily available precursors and a simple phase inversion process. It offers a practical, low-cost alternative to conventional membranes with strong potential for large-scale oil–water separation (Table 3).

The improved performance of PSf membranes after the addition of GO and GO–SiO_2 is closely related to changes in their surface physical and chemical properties. Pure PSf membranes are relatively hydrophobic, allowing oil molecules to readily adsorb onto the surface and clog pores

during the filtration process. This condition results in a significant decrease in flux (high FDR) and limited flux recovery (low FRR). After modification with Graphene Oxide, the membrane surface becomes more hydrophilic due to the presence of oxygen functional groups such as –OH, –COOH, and –O– in the GO structure, which enhances the interaction between water molecules and the membrane surface through hydrogen bonding. This interaction allows the formation of a hydration layer that acts as a dynamic barrier between the oil and the polymer surface, thus preventing fouling buildup and maintaining flux stability during the filtration process.

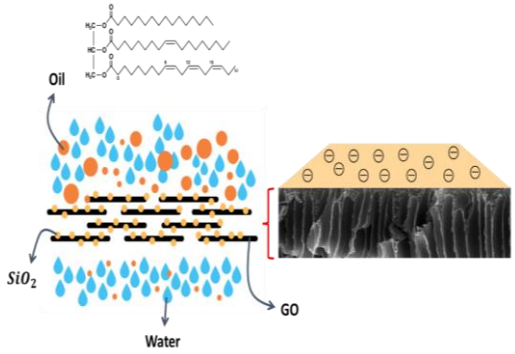

Fig. 13. Illustration of graphene membrane as oil-in-water filtration application.

Furthermore, the incorporation of GO–SiO_2 produces a more pronounced synergistic effect. The well-dispersed SiO_2 particles on the GO sheets expand the hydrophilic surface area and increase the density of silanol groups (–Si–OH), which have a strong affinity for water molecules. The presence of these silanol groups promotes the formation of a stable hydration layer on the membrane surface, while simultaneously enhancing surface hydrophilicity, surface energy, and pore mechanical stability. This synergistic interaction between GO and SiO_2 enables the PSf/GO–SiO_2 (0.6) membrane to exhibit a minimal flux decline (FDR ≈ 4.16%) and a high flux recovery ratio (FRR > 95%), experimentally demonstrating its excellent antifouling characteristics and stable long-term performance. However, excessive addition of SiO_2 can adversely affect membrane performance. An overly high SiO_2 content tends to promote particle agglomeration within the polymer matrix, leading to non-uniform filler distribution and reduced structural integrity of the active layer. This condition can generate larger or irregular pores, decrease separation selectivity, and increase fouling susceptibility due to the formation of surface microdefects. Therefore, although the incorporation of GO–SiO_2 significantly enhances hydrophilic and antifouling properties, optimizing the composition ratio is essential to achieve a proper balance among high permeability, mechanical stability, and effective fouling resistance.

4. Conclusion

This study successfully fabricated and characterized PSf/GO-SiO_2 membranes for oil-in-water filtration. The results showed that variations in TEOS addition affected the membrane pore structure, leading to variations in pore size and macrovoid formation. Membranes containing silica exhibited larger pore sizes and wider macrovoid cavities (SEM), thus enhancing their hydrophilic properties (WCA ≈ 66.24°). However, excessive silica addition resulted in thicker membranes with smaller cavities, indicating that silica concentration plays a significant role in adjusting membrane characteristics. The performance of the PSf/GO-SiO_2 membrane in separating oil particles from water was proven effective. This was supported by the results of membrane performance analysis, which had a small FDR (≈ 4.16%) and FRR (> 95%), indicating that the membrane exhibited excellent and stable antifouling performance. The membrane separation efficiency initially increased with increasing silica content but then decreased due to the widening of the pore size, which affected its filtration ability. These findings highlight the importance of optimizing silica content to achieve desired membrane performance in oil-water separation applications.

Table 3
Differences between different types of membranes and their oil rejection values

Membrane Type	Flux ($L \cdot m^{-2} \cdot h^{-1}$)	FDR (%)	FRR (%)	Cost implication	Ref
Electrospun Nanofiber Membrane	150–250	≈ <10%)	85	High energy, complex process	[41]
Ceramic Membrane	80–150	Low FDR under test conditions	> 90	High, expensive fabrication	[42]
Conventional Psf Uf Membrane	50–120	Tends to experience greater flux reduction unless modified	< 70	Low, widely used	[43]
Psf/GO-SiO_2 (0.6) This Work)	~201.63 (pure water) ~189.43 (water-oil solution)	**≈4.16%** Excellent antifouling performance, increases the hydrophilicity and surface stability against oil.	> 95	Low, scalable fabrication	**This work**

Acknowledgment

The authors gratefully acknowledge the Material Physics Laboratory, Department of Physics, Faculty of Mathematics and Natural Sciences, and the Institute for Research and Community Service, Universitas Negeri Surabaya, for providing facilities that supported this work.

Conflicts of Interest

The authors declare that they have no known competing financial interests or personal relationships that could have appeared to influence the work reported in this paper.

Data availability

The data supporting the findings of this study are included within the article. Additional data are available from the corresponding author upon reasonable request.

Declaration of Competing Interest

The authors declare that they have no known competing financial interests or personal relationships that could have appeared to influence the work reported in this paper.

Credit authorship contribution

N. Munasir: Conceptualization, methodology, data validation, resources, writing-original draft.
A. Anis: Resources, data curation, and investigation.
P. Ariyanti Rasiana: Resources, data curation, data analysis and investigation, and writing-original draft.
F. Nuhaa: Investigation, project administration, software, formal analysis, and writing-review.
S. Ezza Syuhada: Supervision, and proofreading.
T. Ahmad: Writing-review & editing, proofreading, and Turnitin check.

References

[1] H.A. Alalwan, N.S. Mohammed Ali, M.M. Mohammed, M.F. Mohammed, A.H. Alminshid, A comparison study of methyl green removal by peroxi-coagulation and peroxi-electrocoagulation processes, Clean. Eng. Technol. 13 (2023) 100623. https://doi.org/10.1016/j.clet.2023.100623.
[2] A.M. Habl, A.A. Amooey, M.M. Mohammed, H.A. Alalwan, Electro Oxidation Process for Wastewater Treatment in Petroleum Refineries, Pollution 10 (2024) 819–832. https://doi.org/10.22059/poll.2024.371677.2236.
[3] S.K.A. Al-Amshawee, M.Y.B.M. Yunus, H.A. Alalwan, W.H. Lee, F. Dai, Experimental investigation of biofilm carriers of varying shapes, sizes, and materials for wastewater treatment in fixed bed biofilm reactor:

a qualitative study of bio-carrier performance, J. Chem. Technol. Biotechnol. 97 (2022) 2592–2606. https://doi.org/10.1002/jctb.7131.
[4] N.F.D. Junaidi, N.H. Othman, N.S. Fuzil, M.S. Mat Shayuti, N.H. Alias, M.Z. Shahruddin, F. Marpani, W.J. Lau, A.F. Ismail, N.F.D. Aba, Recent development of graphene oxide-based membranes for oil–water separation: A review, Sep. Purif. Technol. 258 (2021) 118000. https://doi.org/10.1016/j.seppur.2020.118000.
[5] H. Yuan, Z. Zhang, Y. Mi, F. Ye, W. Liu, J. Kuan, X. Jiang, Y. Luo, Demulsification of Water-Containing Crude Oil Driven by Environmentally Friendly SiO2@CS Composite Materials, Energy and Fuels 34 (2020) 8316–8324. https://doi.org/10.1021/acs.energyfuels.0c01660.
[6] B. Zhao, L. Ren, Y. Du, J. Wang, Eco-friendly separation layers based on waste peanut shell for gravity-driven water-in-oil emulsion separation, J. Clean. Prod. 255 (2020) 120184. https://doi.org/10.1016/j.jclepro.2020.120184.
[7] N. Munasir, S.R. Lutfiana, F. Nuhaa, S. Evi, R. Lydia, S.S. Ezaa, T. Ahmad, Graphene Based Membrane Modified Silica Nanoparticles for Seawater Desalination and Wastewater Treatment: Salt Rejection and Dyes, Int. J. Eng. Trans. A Basics 36 (2023) 698–708. https://doi.org/10.5829/ije.2023.36.04a.09.
[8] M.B. Alkindy, V. Naddeo, F. Banat, S.W. Hasan, Synthesis of polyethersulfone (PES)/GO-SiO_2 mixed matrix membranes for oily wastewater treatment, Water Sci. Technol. 81 (2020) 1354–1364. https://doi.org/10.2166/wst.2019.347.
[9] S. Kheirieh, M. Asghari, M. Afsari, Application and modification of polysulfone membranes, Rev. Chem. Eng. 34 (2018) 657–693. https://doi.org/10.1515/revce-2017-0011.
[10] Y. Cai, S.Q. Shi, Z. Fang, J. Li, Design, Development, and Outlook of Superwettability Membranes in Oil/Water Emulsions Separation, Adv. Mater. Interfaces 8 (2021) 1–30. https://doi.org/10.1002/admi.202100799.
[11] A. Kusumaatmaja, N. Fauji, K. Triyana, Polysulfone/polyacrilonitrile membrane for oil/water separation, Mater. Sci. Forum 886 MSF (2017) 145–149. https://doi.org/10.4028/www.scientific.net/MSF.886.145.
[12] Z. Wu, C. Zhang, K. Peng, Q. Wang, Z. Wang, Hydrophilic/underwater superoleophobic graphene oxide membrane intercalated by TiO_2 nanotubes for oil/water separation, Front. Environ. Sci. Eng. 12 (2018). https://doi.org/10.1007/s11783-018-1042-y.
[13] Y. Wei, H. Qi, X. Gong, S. Zhao, Especially Wettable Membranes for Oil–Water Separation, Adv. Mater. Interfaces 5 (2018) 1–27. https://doi.org/10.1002/admi.201800576.
[14] F. Ebrahimi, S.R. Nabavi, A. Omrani, Fabrication of hydrophilic special sandwich structure of PAN/GO/SiO_2 electrospun membrane decorated with SiO2 nanoparticles for oil/water separation, J. Water Process Eng. 48 (2022) 102926. https://doi.org/10.1016/j.jwpe.2022.102926.
[15] Y. Liu, F. Zhang, W. Zhu, D. Su, Z. Sang, X. Yan, S. Li, J. Liang, S.X. Dou, A multifunctional hierarchical porous SiO_2/GO membrane for high efficiency oil/water separation and dye removal, Carbon N. Y. 160 (2020) 88–97. https://doi.org/10.1016/j.carbon.2020.01.002.
[16] J. Hwang, J. Choi, J.M. Kim, S.W. Kang, Water treatment by polysulfone membrane modified with tetrahydrofuran and water pressure, Macromol. Res. 24 (2016) 1020–1023. https://doi.org/10.1007/s13233-016-4145-y.
[17] H.T.V. Nguyen, T.H.A. Ngo, K.D. Do, M.N. Nguyen, N.T.T. Dang, T.T.H. Nguyen, V. Vien, T.A. Vu, Preparation and characterization of a hydrophilic polysulfone membrane using graphene oxide, J. Chem. 2019 (2019) 15–20. https://doi.org/10.1155/2019/3164373.
[18] M.E.A. Ali, A. Shahat, T.I. Ayoub, R.M. Kamel, Fabrication of high flux polysulfone/mesoporous silica nanocomposite ultrafiltration membranes for industrial wastewater treatment, Biointerface Res. Appl. Chem. 12 (2022) 7556–7572. https://doi.org/10.33263/BRIAC126.75567572.
[19] Y. Zhu, D. Wang, L. Jiang, J. Jin, Recent progress in developing advanced membranes for emulsified oil/water separation, NPG Asia Mater. 6 (2014). https://doi.org/10.1038/am.2014.23.
[20] R.S. Zambare, K.B. Dhopte, P.R. Nemade, C.Y. Tang, Effect of oxidation degree of GO nanosheets on microstructure and performance of polysulfone-GO mixed matrix membranes, Sep. Purif. Technol. 244 (2020) 116865. https://doi.org/10.1016/j.seppur.2020.116865.
[21] A. Sjahriza, S. Herlambang, Sintesis Oksida Grafena dari Arang Tempurung Kelapa Untuk Aplikasi Antibakteri dan Antioksidan, Al-Kimiya 8 (2021) 51–58. https://doi.org/10.15575/ak.v8i2.13473.
[22] M. Nasir, Y.P. Utami, N. Faaizatunnisa, L. Rohmawati, E. Suebah, A. Taufiq, E.S. Sazali, The GO-Fe_3O_4/Psf Membrane Prepared by Phase Inversion for Filtration: Dyes and NaCl in Water, J. Water Environ. Nanotechnol. 8 (2023) 241–253. https://doi.org/10.22090/JWENT.2023.03.004.
[23] A.S. Purwanto, T. Taslimah, S. Sriatun, Sintesis dan Karakterisasi Silica Gel dari Tetraetilortosilikat (TEOS) Menggunakan Surfaktan Polyethylene Glycol (PEG) 6000 dalam Kondisi Basa, J. Kim. Sains Dan Apl. 15 (2012) 1–6. https://doi.org/10.14710/jksa.15.1.1-6.
[24] I.Y. Wani, K. Singh, Effect of encapsulated bacteria on concrete properties: A review, Mater. Today Proc. 33 (2019) 1706–1712. https://doi.org/10.1016/j.matpr.2020.07.540.
[25] X. Li, J. Huang, Y. Zhang, Y. Lv, Z. Liu, Z. Shu, Characterization and antifouling performance of negatively charged PES/mesoporous silica ultrafiltration membrane for raw water filtration, Desalin. Water Treat. 57 (2016) 10980–10987. https://doi.org/10.1080/19443994.2015.1043651.
[26] H. Wu, B. Tang, P. Wu, Development of novel SiO_2-GO nanohybrid/polysulfone membrane with enhanced performance, J. Memb. Sci. 451 (2014) 94–102. https://doi.org/10.1016/j.memsci.2013.09.018.
[27] Y. Huang, H. Jin, P. Yu, Y. Luo, Polyamide thin-film composite membrane based on nano-silica modified polysulfone microporous support layer for forward osmosis, Desalin. Water Treat. 57 (2016) 20177–20187. https://doi.org/10.1080/19443994.2015.1108874.
[28] W. Angesti, M. Munasir, Fabrication and Characterization of Polysulfone Membrane Based On GO-SiO2 Composite using Phase Inversion Method, E3S Web Conf. 328 (2021). https://doi.org/10.1051/e3sconf/202132801010.
[29] R. Dong, L. Wang, J. Zhu, L. Liu, Y. Qian, A novel SiO_2-GO/ acrylic resin nanocomposite: fabrication, characterization and properties, Appl. Phys. A (2019). https://doi.org/10.1007/s00339-019-2847-7.
[30] L. Feng, Y. Gao, Y. Xu, H. Dan, Y. Qi, S. Wang, F. Yin, Q. Yue, B. Gao, A dual-functional layer modified GO@SiO_2 membrane with excellent anti-fouling performance for continuous separation of oil-in-water emulsion, J. Hazard. Mater. 420 (2021) 1–13. https://doi.org/10.1016/j.jhazmat.2021.126681.
[31] M. Nasir, N. Faaizatunnisa, N.M. Ariesta, L. Rohmawati, R.A. Nurazizah, Facile in situ synthesis and characterization of Fe@Si/zeolite Na composites with magnetic core–shell structures from natural materials for enhanced curcumin loading capacity, Nanotechnol. Precis. Eng. 7 (2024). https://doi.org/10.1063/10.0025584.
[32] L. Shen, W. Hu, Z. Lei, J. Peng, E. Zhu, X. Zhang, M. Yang, X. Feng, Y. Yang, Y. Mi, Nanoscale silica-coated graphene oxide and its demulsifying performance in water-in-oil and oil-in-water emulsions, Environ. Sci. Pollut. Res. 28 (2021) 55454–55464. https://doi.org/10.1007/s11356-021-14888-1.
[33] R. Rezaee, S. Nasseri, A.H. Mahvi, R. Nabizadeh, S.A. Mousavi, A. Maleki, M. Alimohammadi, A. Jafari, S. Hemmati Borji, Development of a novel graphene oxide-blended polysulfone mixed matrix membrane with improved hydrophilicity and evaluation of nitrate removal from aqueous solutions, Chem. Eng. Commun. 206 (2019) 495–508. https://doi.org/10.1080/00986445.2018.1503174.
[34] S. Mallakpour, M. Naghdi, Polymer/SiO_2 nanocomposites: Production and applications, 2018. https://doi.org/10.1016/j.pmatsci.2018.04.002.
[35] D. Rakhmawaty, A. Rostika, D. Janati, Sintesis Silika Metode Sol-Gel Sebagai Penyangga Fotokatalis TiO_2 Terhadap Penurunan Kadar Kromium dan Besi, J. Sains Mater. Indones. 17 (2016) 82–89.
[36] A. Alkhouzaam, H. Qiblawey, Novel polysulfone ultrafiltration membranes incorporating polydopamine functionalized graphene oxide with enhanced flux and fouling resistance, J. Memb. Sci. 620 (2021) 118900. https://doi.org/10.1016/j.memsci.2020.118900.
[37] M. Fadli, A. Khausar, S. Sofyana, U. Fathanah, Karakteristik Membran Komposit Polietersulfon, Polivinilpirolidon dan Kitosan, J. Serambi Eng. 6 (2021) 2310–2319. https://doi.org/10.32672/jse.v6i4.3476.
[38] F.R. Hikmawan, E. Evitasari, G.A. Bintan Sukono, D. Satriawan, Teknologi Membran Untuk Pengolahan Emulsi Minyak: Review, J. Pengendali. Pencemaran Lingkung. 2 (2020) 25–32. https://doi.org/10.35970/jppl.v2i2.348.
[39] U. Fathanah, H. Meilina, Karakterisasi dan Kinerja Membran Polyethersulfone Termodifikasi Aditif Anorganik secara Blending Polimer, J. Serambi Eng. 6 (2021) 2407–2414. https://doi.org/10.32672/jse.v6i4.3515.
[40] M. dan C.K. Widyasmara, Potensi Membran Mikrofiltrasi Dan Ultrafiltrasi Untuk Pengolahan Limbah Cair Berminyak, J. Teknol. Kim. Dan Ind. 2 (2013) 295–307.
[41] X. Cheng, T. Li, L. Yan, Y. Jiao, Y. Zhang, K. Wang, Z. Cheng, J. Ma, L. Shao, Biodegradable electrospinning superhydrophilic nanofiber membranes for ultrafast oil-water separation, Sci. Adv. 9 (2023). https://doi.org/10.1126/sciadv.adh8195.
[42] A. Avornyo, A. Thanigaivelan, R. Krishnamoorthy, S.W. Hassan, F. Banat, Ag-CuO-Decorated Ceramic Membranes for Effective Treatment of Oily Wastewater, Membranes (Basel). 13 (2023). https://doi.org/10.3390/membranes13020176.

[43] H.M. Mousa, H.S. Fahmy, G.A.M. Ali, H.N. Abdelhamid, M. Ateia, Membranes for Oil/Water Separation: A Review, Adv. Mater. Interfaces 9 (2022) 1–36. https://doi.org/10.1002/admi.202200557.
[44] M.J. Li, C.M. Liu, Y.B. Xie, H. Bin Cao, H. Zhao, Y. Zhang, The evolution of surface charge on graphene oxide during the reduction and its application in electroanalysis, Carbon N. Y. 66 (2014) 302–311. https://doi.org/10.1016/j.carbon.2013.09.004.
[45] Y.C. Woo, S.H. Kim, H.K. Shon, L.D. Tijing, Introduction: Membrane desalination today, past, and future, Elsevier Inc., (2018). https://doi.org/10.1016/B978-0-12-813551-8.00028-0.
[46] S. Karakaya, Ş. Şimşek, Changes in total polar compounds, peroxide value, total phenols and antioxidant activity of various oils used in deep fat frying, JAOCS, J. Am. Oil Chem. Soc. 88 (2011) 1361–1366. https://doi.org/10.1007/s11746-011-1788-x.